Climate change impacts on streamflow at the upper Jordan River based on an ensemble of regional climate models

A. Givati, Guillaume Thirel, D. Rosenfeld, D. Paz

Journal of Hydrology: Regional Studies 21 (2019) 92–109

Contents lists available at ScienceDirect

Journal of Hydrology: Regional Studies

journal homepage: www.elsevier.com/locate/ejrh

Climate change impacts on streamflow at the upper Jordan River based on an ensemble of regional climate models

Amir Givati[a,*], Guillaume Thirel[b], Daniel Rosenfeld[c], Dror Paz[d]

[a] Israeli Hydrological Service, Israel
[b] IRSTEA, HYCAR research unit, Antony, France
[c] The Hebrew University of Jerusalem,Jerusalem, Israel
[d] Israeli Hydrological Service, Israel

ARTICLE INFO

Keywords:
Rainfall - runoff relationships
Ensemble of regional climate models
Changes in the hydrological cycle

ABSTRACT

Study Region: The upper Jordan River is the major water resource in Israel, a country which suffers from increasing shortage of natural water resources.
Study Focus: In this study, we apply for the first time to this area an approach based on an ensemble of regional climate models, verify their trends vs. observations for a control period and use them for simulating future discharges of the Jordan River.
New Hydrological Insights for the Region: The results of this study show that the observed negative trend of precipitation for the control period is also simulated by the climate models ensemble and projects a continued decreasing trend to the near future and further into the far future. Using the GR6J daily hydrological model for evaluating the effects of the predicted climate changes on the hydrological cycle in the region shows an increase in potential evaporation and a decrease in streamflow volumes in the Jordan River, Northern Israel. The results reveal and quantify the changes in rainfall–runoff relationships. These changes in the hydrological cycle in the region can be explained by changes in precipitation distribution and duration and decrease in soil moisture caused by the increase in evaporation. Results presented in this study could imply major consequences for the region. The findings here are relevant not only to Israel but also to the surrounding countries.

1. Introduction

The expected impacts of climate change in the Eastern Mediterranean and Middle East region are worrying. The most recent IPCC general circulation models (GCMs) projections agree on drying scenarios in the region by the end of the 21st century (IPCC, 2013). Future climate in the region is expected to be characterized by possible decreasing precipitation and increasing temperature trends (Kunstmann et al., 2007; Krichak et al., 2010; Peleg et al., 2015; Samuels et al., 2017). These future evolutions impact a region that is already affected by sparse water resources (Evans, 2009; Chenoweth et al., 2011; Smiatek et al., 2011; Kelley et al., 2015). A significant decrease in rainfall, spring flow and streamflow has recently been documented both in the Jordan River basin in Northern Israel (Givati and Rosenfeld, 2007; Rimmer et al., 2011) as well as in the Litani River basin in Lebanon (Shaban, 2009). The average available water (natural recharge minus evaporation) in Lake Kinneret decreased to 392 mcm/year for the period 1975–2010 to 365 mcm/year for the period 1985–2010 and down to 319 mcm/year for the period 1993–2010 (Rimmer and Givati, 2014). Fig. 1

* Corresponding author at: Israeli Hydrological Service, Jerusalem, POB 36118, Israel.
E-mail address: amirg@water.gov.il (A. Givati).

https://doi.org/10.1016/j.ejrh.2018.12.004
Received 27 June 2018; Received in revised form 18 December 2018; Accepted 18 December 2018

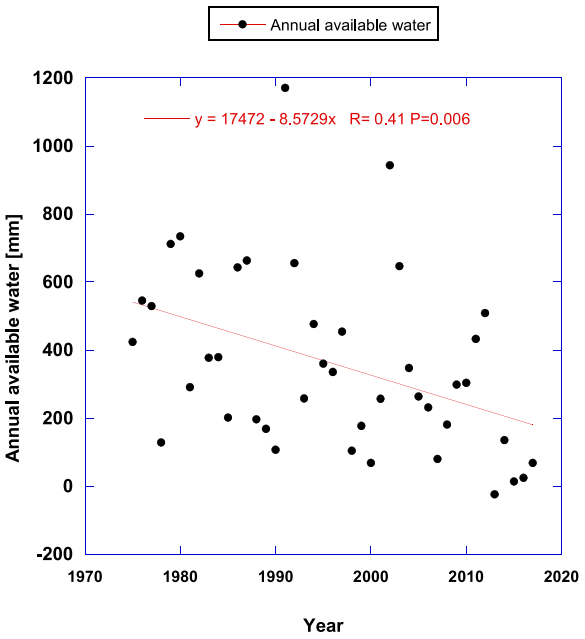

Fig. 1. Annual available water in Lake Kinneret.

shows a statistically significant (P = 0.006) decreasing trend in the available water volumes entering into lake Kinneret for the period 1975–2017 (available water volumes are defined as the total incoming water to lake from direct precipitation, streamflow and springs minus the evaporation from the lake).

Future hydroclimate projections are extremely important for operational stakeholders and for planning the water sector in this region. There is a growing need for hydrological simulations at the basin scale, in order to better plan the future water allocation. GCMs are relatively coarse (~100-200 km grid resolution) and are incapable of resolving the necessary details of the complex precipitation structures that are forced by mesoscale orography, land-surface heterogeneities and land-water contrasts. In the Eastern Mediterranean region, strong sea-air interactions and orographic forcing produce precipitation with strong gradients that are generally missed by the coarse-grid operational models. In Israel, the precipitation patterns are particularly complex and large precipitation contrasts occur over a relatively small geographical distance. Large climatological precipitation gradients in Israel are caused by the complex orography and the coastline shape (Saaroni et al., 2009).

To cope with these limitations, downscaling of GCMs outputs is necessary. The downscaling can be realized through the use of regional climate models (RCMs) that are limited-area models constrained by the GCMs outputs. Analyses confirm the ability of RCMs to capture the basic features of the climate at the Euro-Cordex domain, including its variability in space and time (Kotlarski et al., 2014).

Moreover, climate change impact needs to be assessed at regional and local scales. This requires climate projection information at a spatial scale relevant to the system of interest, which is often significantly smaller than the resolution of GCMs. Dynamic downscaling with RCMs is capable to address this scale gap. A number of previous projects have produced regional climate projections using RCM ensembles including PRUDENCE (Kotlarski et al., 2014), ENSEMBLES (van der Linden and Mitchell, 2009), RMIP (Fu et al., 2005), NARCCAP (Mearns et al., 2012), CLARIS-LPB (Solman et al., 2013). In each case, various strategies were used to design the experimental procedure in order to sample the model uncertainties, which are driven by practical limitations of computation time and data storage. The highest possible accuracy of climate projections (precipitation, temperatures) is needed for hydrological projections, including the Eastern Mediterranean and Middle East. In order to support the decision makers, studies have to address a range of future hydroclimate scenarios while identifying the most likely one.

Here we propose a new methodology that uses the output of an ensemble of regional climate models as input to hydrological modeling, and apply the outcome to the upper Jordan River for predicting future water volumes and discharges. We used daily precipitation and temperature from the various climate models provided by CORDEX (after verifying each of them vs. the observed precipitation trend) as an input for the hydrological simulation, and obtain the streamflow at the Jordan River. In addition to the hydrological simulations based on individual climate models, we used the average of the 19 outputs, which constitutes the ensemble mean. Each member was represented with an identical weight in the ensemble. Previous studies have already shown the advantages of using ensemble of climate models for hydrological applications in Israel (Givati et al., 2017).

Various hydrological models can be used in order to translate climate input data into water volumes. We used in this study the GR6J daily lumped conceptual rainfall-runoff model in order to assess the impact of climate change on river streamflow. Such hydroclimate simulations were not done yet in the Eastern Mediterranean. Their ensemble results will give water resources mangers and planners in the region new tools to evaluate and plan accordingly in response to expected changes in the hydrological cycle and water

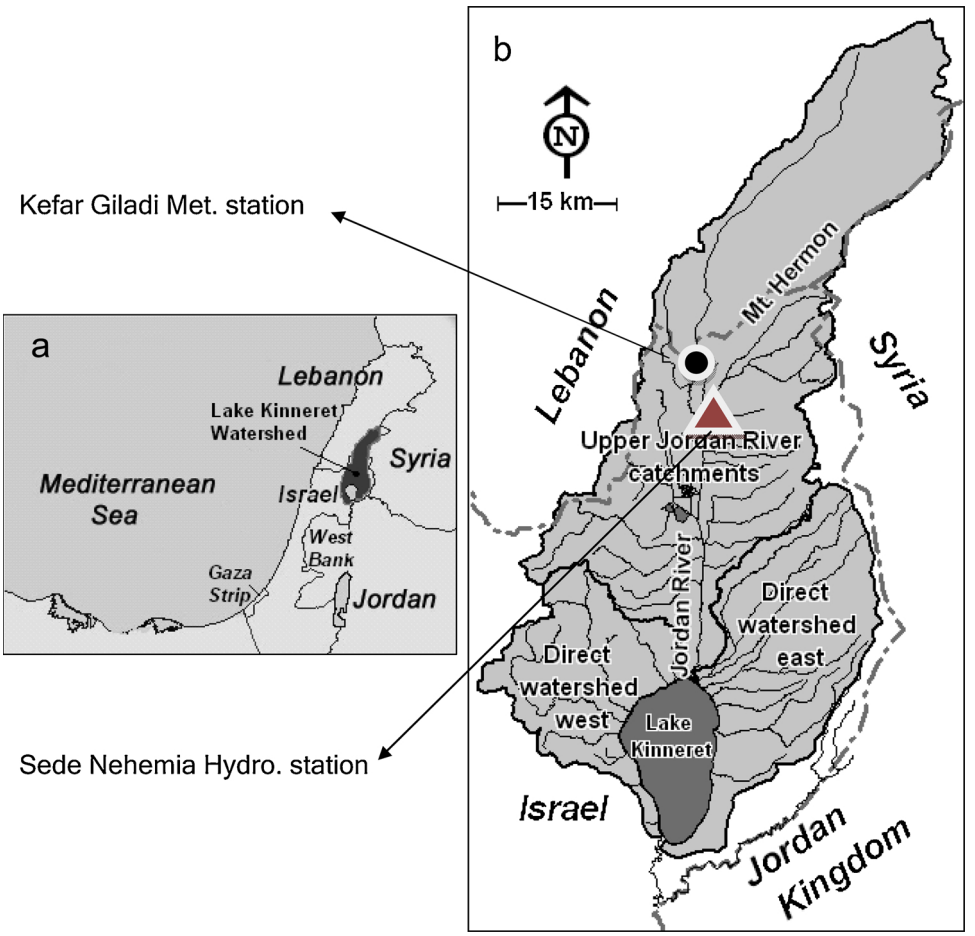

Fig. 2. Maps of study area: (a) the Eastern Mediterranean; (b) Lake Kinneret watershed of the Upper catchments of the Jordan River and the location of Kefar Giladi rain gauge (in Black circle).

Table 1
The general circulation models and the Cordex regional climate models.

Model Domain	RCM	GCM	Resolution [degrees]
EURO – Cordex	CLMcom-CCLM	CNRM-CERFACS	0.11
EURO – Cordex	CLMcom-CCLM	ICHEC-EC-EARTH	0.11
EURO – Cordex	SMHI	ESM-LR	0.11
MENA – Cordex	CLMcom-CCLM	MPI-ESM_IMS	0.44
MENA – Cordex	WRF	CESM	0.44
Africa – Cordex	CLMcom-CCLM	CNRM	0.44
Africa – Cordex	CLMcom-CCLM	ICHEC	0.44
Africa – Cordex	CLMcom-CCLM	MOHC	0.44
Africa – Cordex	DMI	ICHEC	0.44
Africa – Cordex	KNMI	ICHEC	0.44
Africa – Cordex	KNMI	MOHC	0.44
Africa – Cordex	SMHI	CCMA	0.44
Africa – Cordex	SMHI	CNRM	0.44
Africa – Cordex	SMHI	ICHEC	0.44
Africa – Cordex	SMHI	MIROC	0.44
Africa – Cordex	SMHI	MOHC	0.44
Africa – Cordex	SMHI	MPI	0.44
Africa – Cordex	SMHI	NCC	0.44
Africa – Cordex	SMHI	NOAA	0.44

Table 2
Precipitation slope [mm/y] and the Student *t*-test for each model at the control period.1951–2005

Model Domain	RCM	GCM	Precipitation Slope 1951-2005 [mm/y]	T diff
Kefar Giladi–Observed			−0.14	
Ensemble mean			−0.16	+0.01
EURO – Cordex	CLMcom-CCLM	MOHC-HadGEM2	−0.40	−0.11
EURO – Cordex	KNMI-RACMO	MOHC-HadGEM2-ES	−0.67	−0.21
EURO – Cordex	CLMcom-CCLM	MPI-M-MPI-ESM-LR	−3.37	−0.29
MENA – Cordex	CLMcom-CCLM	MPI-ESM	−6.56	+2.42
MENA – Cordex	WRF	CESM	−0.39	+0.13
Africa – Cordex	CLMcom-CCLM	CNRM	−1.51	+0.52
Africa – Cordex	CLMcom-CCLM	ICHEC	+0.72	+0.30
Africa – Cordex	CLMcom-CCLM	MOHC	+4.15	+1.38
Africa – Cordex	DMI	ICHEC	−2.27	+0.79
Africa – Cordex	KNMI	ICHEC	−1.24	+0.46
Africa – Cordex	KNMI	MOHC	+2.02	+0.85
Africa – Cordex	SMHI	CCMA	+1.16	+0.54
Africa – Cordex	SMHI	CNRM	−3.51	+1.17
Africa – Cordex	SMHI	ICHEC	−0.50	+0.14
Africa – Cordex	SMHI	MIROC	−1.38	+0.51
Africa – Cordex	SMHI	MOHC	+3.05	+1.10
Africa – Cordex	SMHI	MPI	−2.33	+0.83
Africa – Cordex	SMHI	NCC	+1.04	+0.42
Africa – Cordex	SMHI	NOAA	−1.32	+0.42

availability under various climate-hydrological scenarios. The range of scenarios is based on the IPCC emission scenarios. This study is also trying to evaluate changes in rainfall – runoff relationship in order to better understand the effects of climate change on the hydrological cycle.

2. Methodology and study area

2.1. The study area

The study area is the upper Jordan River basin in Northern Israel (Fig. 2). The climate conditions in the basin change sharply from North to South; while the North is relatively wet with annual precipitation around 800–1000 mm/y in the mountain regions and provides most the of water resources of the basin, the southern part covers lower elevations (the Lake Galilee is located at -210 masl) and is drier (annual precipitation is less than 400 mm/y). The region's climate is strongly affected by external forcing of both mid latitude and tropical origins (Alpert et al., 2005). Most of the annual precipitation is obtained during a limited number of rainy days (45 to 60 days). The rainy events are typically associated with intrusions of cold air masses with a North-European origin that pass over the Mediterranean Sea. Topography and coastal features (with windward effects, gap winds, land-sea breezes) also influence the spatial distribution of climate characteristics in the region (Krichak et al., 2010).

Observed meteorological forcing (daily precipitation and temperatures) was available from the Kefar Giladi Israeli meteorological station. Daily observed discharge data from the Sede Nehamia Israeli Hydrological Service hydrometric station at the Jordan River head water was used. The station drains an area of 800 km^2 and the annual average streamflow volume is 360 mcm for the period 1979–2005 (see the station location on Fig. 2). The potential evapotranspiration that was used for the rainfall-runoff model was computed with the use of the Oudin's formula (Oudin et al., 2005), implemented in the airGR package (Coron et al., 2017b).

2.2. The Cordex data base: Ensemble of regional climate models

Nineteen daily regional climate models (RCMs) from the CORDEX project were used in this study for the control and future simulations (for future simulations at RCP 8.5 scenario we had to use only 17 models due to partial data). We used models from Africa, Middle East-North Africa (MENA) and Euro CORDEX domains that contain simulations based on observed emission for the period 1951–2005 and future simulations based on future emission scenarios for the period 2006–2080 for two IPCC radiative concentration pathways (RCPs): RCP4.5 (reduced CO_2 emissions after 2040) and RCP8.5 (business as usual). The data from the models were extracted for a chosen location at the upper part of the Jordan River basin (Lat.: 33.240/ Long.: 35.596 see location at Fig. 2, in the black circle, Kefar Giladi meteorological station). The data set contains daily time series for precipitation and temperature. The period from 1951 until 2005 was defined as control period and from 2006 the simulations were based on the different RCPs. We analyzed the full 1951–2005 period for long-term trends of observed and projected climate and then compared to around 30 years of simulation: 1979–2005 as the control period vs. the future periods of 2020–2049 (near future) and 2050–2079 (far future).

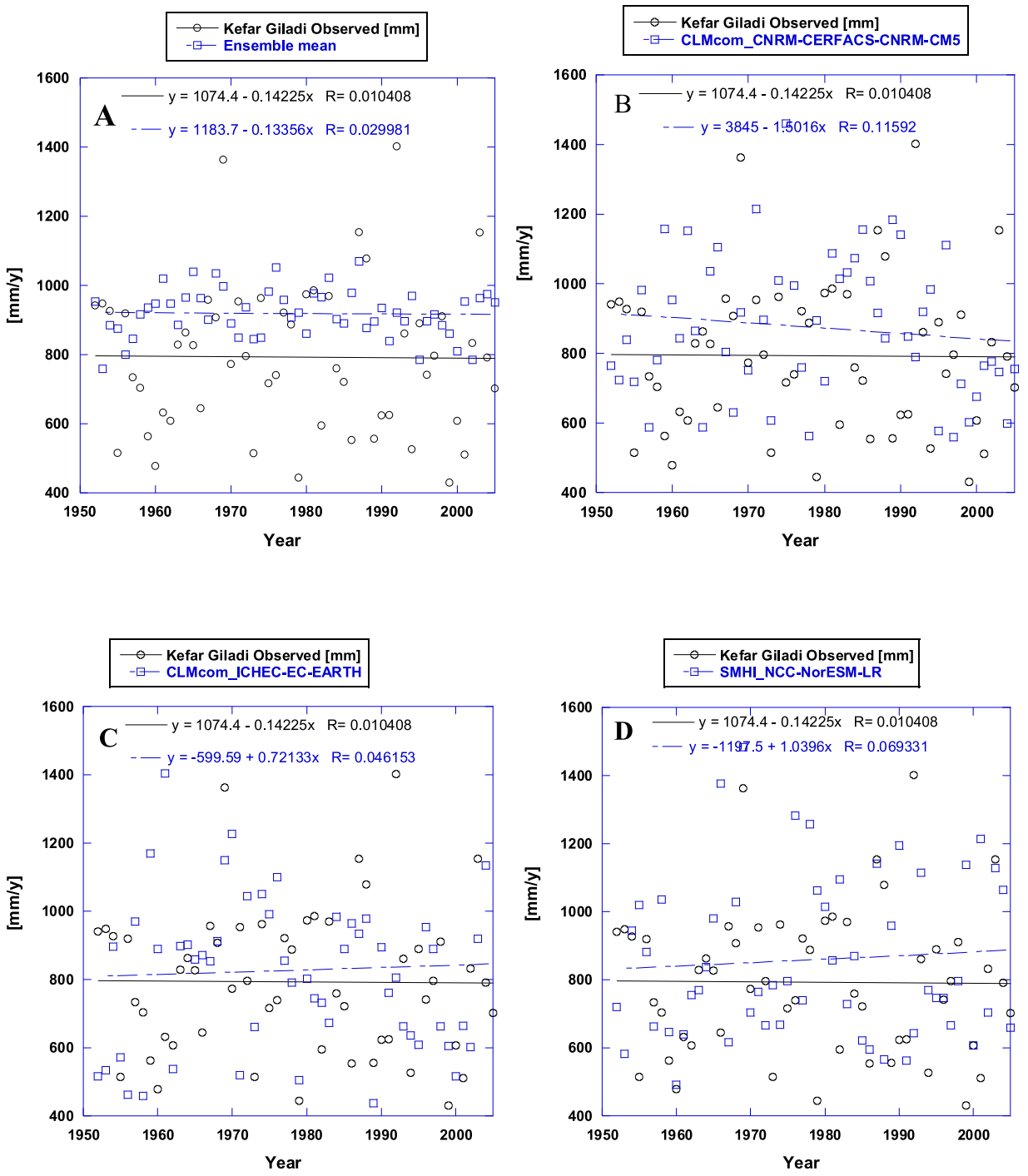

Fig. 3. Annual precipitation and trends at Kefar Giladi station. Ensemble mean of simulated precipitation from 19 regional climate models based on Cordex Africa and Mena (A) and each member in the ensemble (B to S).

Fourteen models of the CORDEX data base were from the Africa CORDEX domain, 3 from EURO CORDEX and 2 from MENA CORDEX (one RCM was provided by the Israeli Meteorological Service and the other by the Cyprus institute, Zittis et al., 2014). The list of GCMs and the details regarding the Cordex different RCMs are provided in Table 1.

Since the climate data from the various models are used to simulate the future hydrological conditions with respect to the current ones (for example the average water volume amounts at the Jordan River for the period 2020–2050 with respect to the average

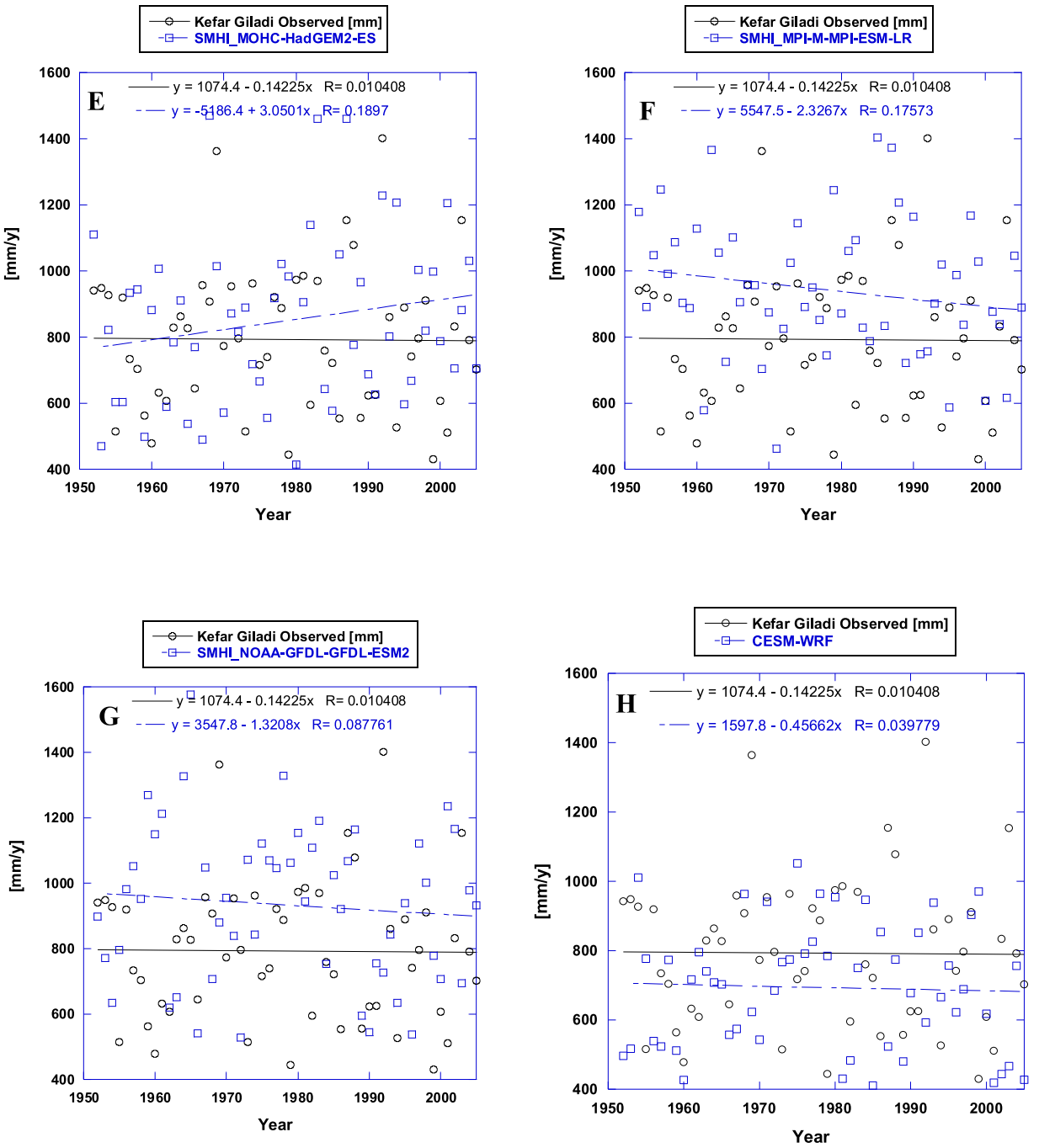

Fig. 3. (*continued*)

volumes at the period 1979–2005), there is a need to evaluate first each RCM performance with respect to observed values. In order to do it we calculated the annual precipitation trends for the period 1951–2005. The trend was calculated for each individual RCM and for the RCM ensemble mean. The RCMs trend was compared to the observed precipitation trend at Kefar Giladi meteorological station, the closest location to the models grid point extraction (see Fig. 2). A Student's *t*-test was used in order to evaluate the significance of each model trend with respect to the observed precipitation trend (a parametric method for normal distribution annual precipitation data set). The assumption behind this methodology is that if a model was able to reconstruct well the observed precipitation trend, it allows us to consider using it for the future simulations. Good performance of a model/ensemble for the control

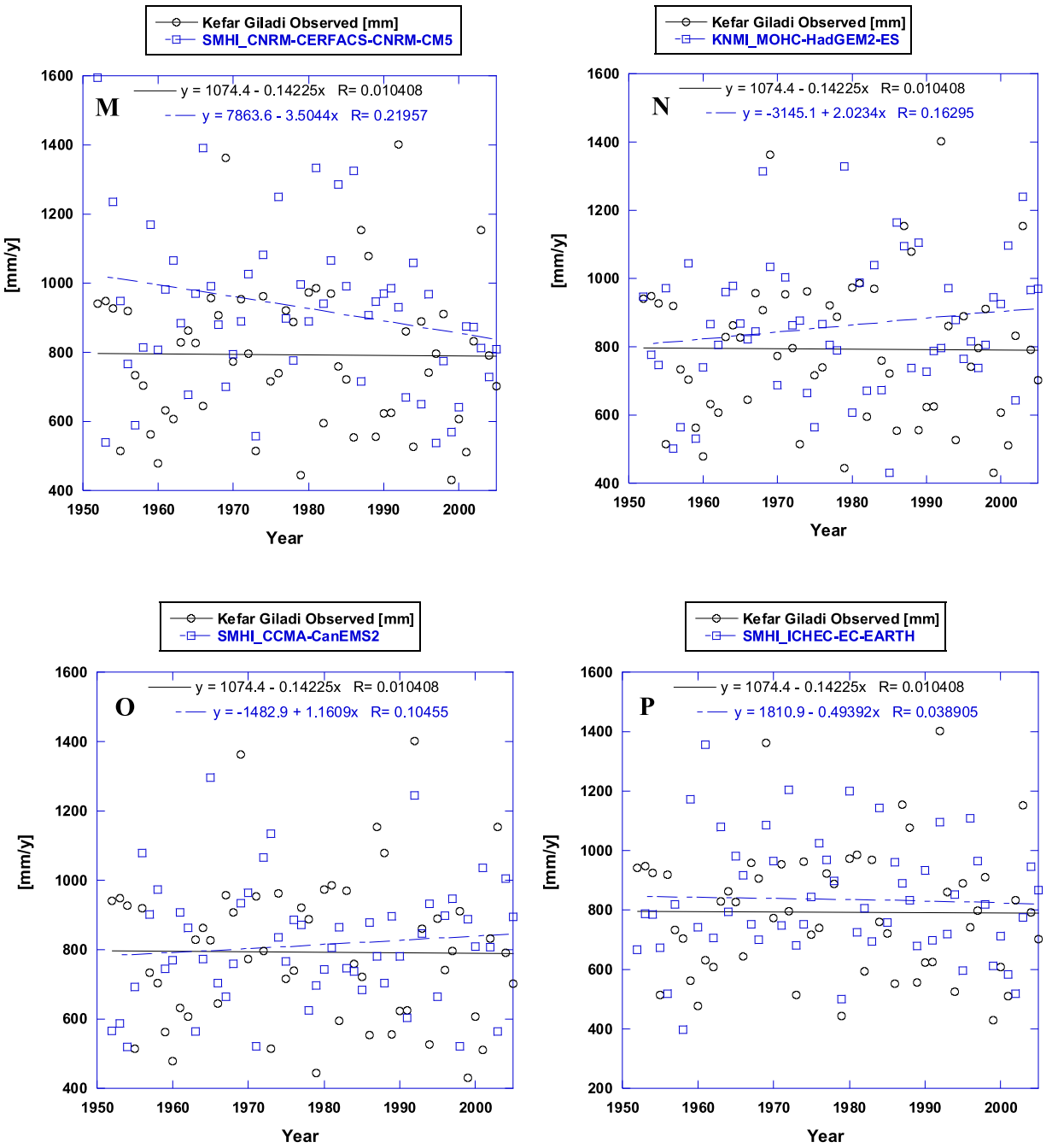

Fig. 3. (*continued*)

period still does not assure that this will be also the case in the future. It can only allow us to assume that the model results for the control period are indicating a suitable model physics which can give some more credibility for the future simulation.

Annual precipitation data are important for the models long-term trend analysis; however, monthly resolution is also essential for evaluating the models seasonality and precipitation variability. Bias in monthly precipitation distribution in a model with respect to the observed (for example, simulated compared to the observed precipitation of the dry seaso, which is the summer), means unresolved model physics and would make it difficult to trust the simulations for the future. In addition, bias in monthly precipitation would directly lead to bias in the hydrological simulation.

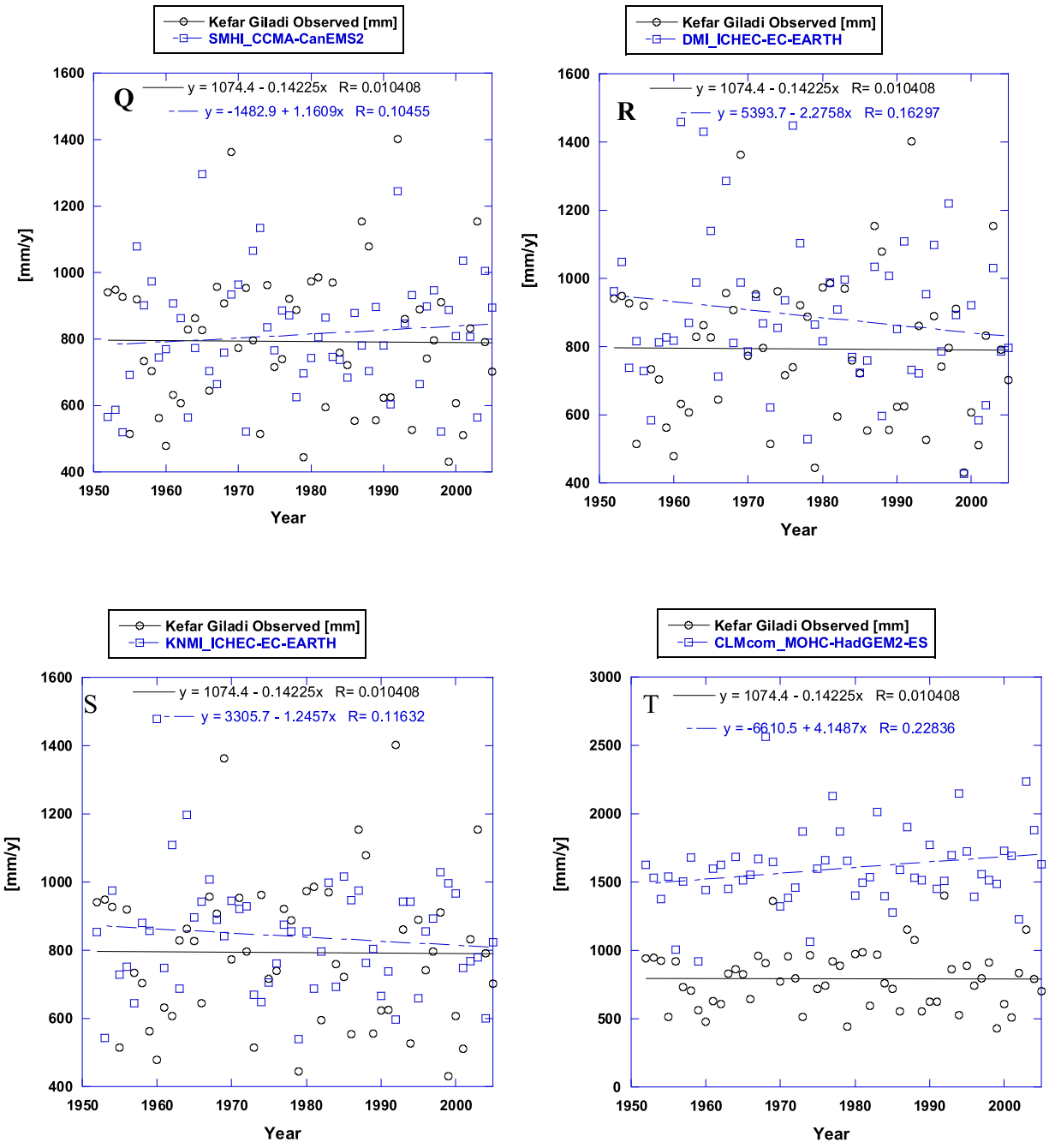

Fig. 3. (*continued*)

In order to examine the climate models seasonality behavior, we plotted the monthly precipitation averages of each model and the ensemble mean vs. the observed precipitation values in Kefar Giladi rain gauge for the period 1951–2005.

The post processing of the climate model data included statistical downscaling for the precipitation and temperature daily data using the quintile mapping methodology for bias correction. No climate model was excluded from the ensemble.

2.3. Hydrological simulations using the GR6J rainfall-runoff model

Assessing the impact of climate change on river streamflow requires the use of rainfall-runoff models, i.e. models transforming climatic time series into streamflow time series. In this study, the daily lumped conceptual GR6J model was used. It was chosen

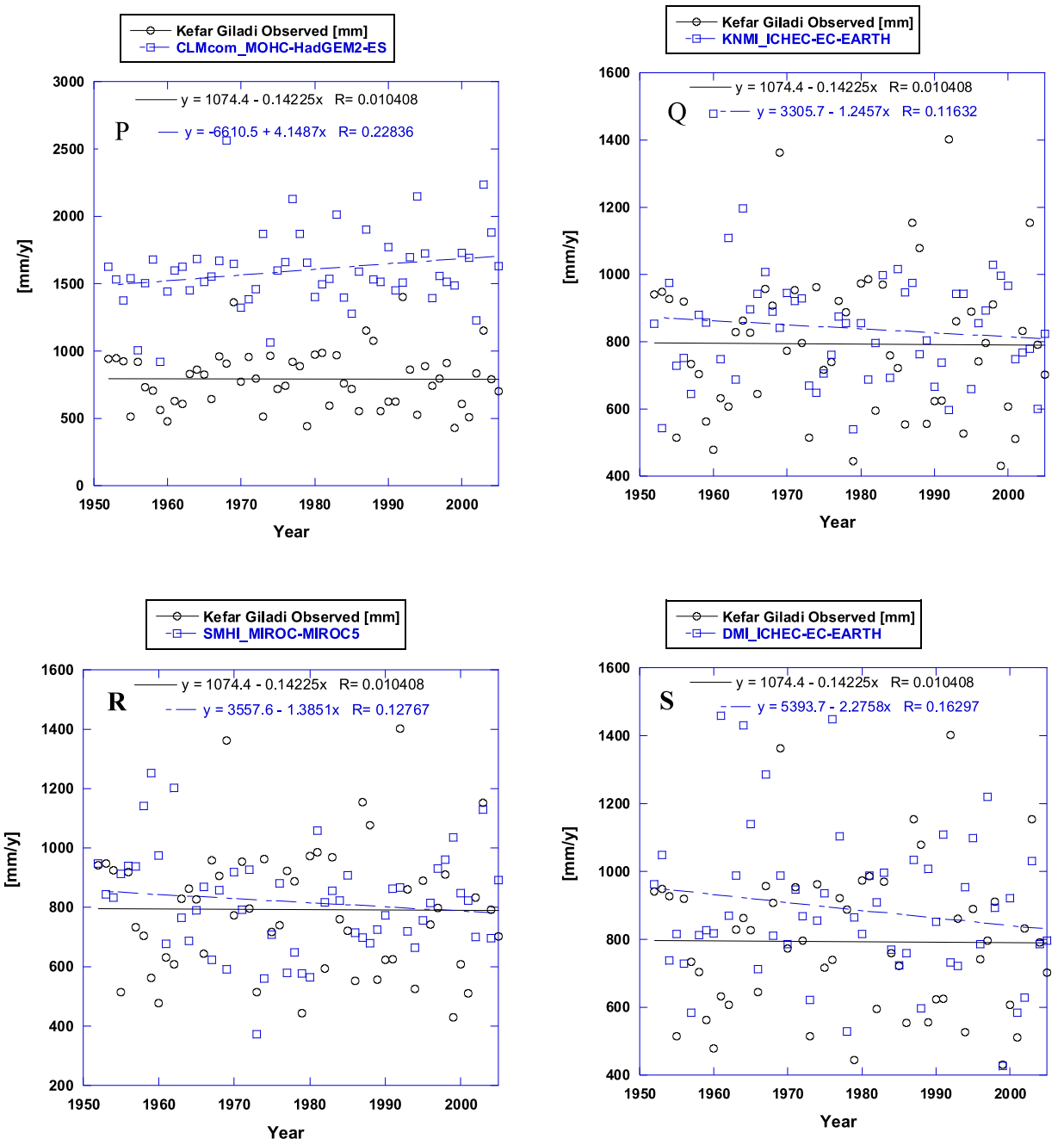

Fig. 3. (*continued*)

because of its ability to reproduce well high as well as low flows (Pushpalatha et al., 2011). The GR6J model is a storage type model that has six free parameters to calibrate. The GR6J requires daily precipitation and potential evapotranspiration input time series. The potential evapotranspiration input was calculated using the Oudin formulation (Oudin et al., 2005). The GR6J model and the Oudin potential evapotranspiration were used within the airGR version 1.5.0.12 R package (Coron et al., 2017a, b).

The robustness of hydrological models, i.e. their ability of being applied to different periods or basins, is crucial for applications to changing conditions (Thirel et al., 2015). In this work, a calibration-validation exercise was undertaken: an automatic calibration algorithm was used to find the combination of parameters that lead to the best simulations of discharge (i.e. simulated discharge closest to observed discharge).

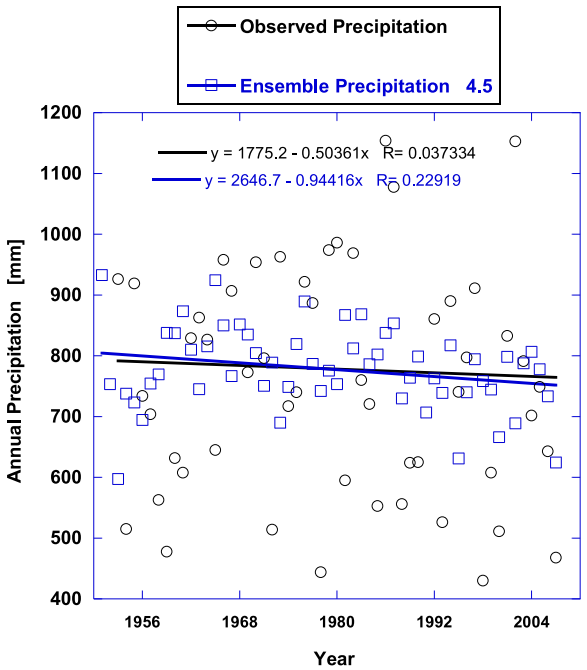

Fig. 4. Simulated annual precipitation from all models (ensemble mean, in blue) vs. the observed precipitation in Kefar Giladi, Kinnert basin for the control period of 1951–2005.

Calibration was performed over the period 1981–1987 and an independent validation was made over the period 1988–2014. For this exercise, we used the observed meteorological forcing from the Kefar Giladi Israeli meteorological station (a station with a full daily data set of precipitation and temperature for the entire calibration and validation periods). The model calibration was done against observed daily discharge data from the Sede Nehamia Israeli Hydrological Service hydrometric station.

An expected feature of the rainfall-runoff model is to provide good quality simulations over the validation period. Indeed, this shows the robustness of the model, i.e. its temporal transferability, which is a necessary quality especially for climate change impact applications (Klemeš, 1986; Thirel et al., 2015).

To assess the quality of the simulations, we used both numerical criteria and visual inspection. The main criterion that we used is the KGE' (Kling et al., 2012), which is a combination of the bias ratio, the correlation coefficient and the coefficient of variation. In addition, the Nash-Sutcliffe Efficiency (NSE, Nash and Sutcliffe, 1970) was used for an evaluation purpose only.

The next step after running the model for the calibration and validation periods with observed meteorological data set was to produce hydrological projections for the periods 1979–2005 and 2020–2080 using the different 19 climate projections for both RCP4.5 and RCP8.5 used as inputs. The annual streamflow volume at the upper Jordan River was calculated for each simulation, and also for the ensemble in both RCP scenarios. In addition to the daily precipitation inputs, we analyzed the daily simulated potential evaporation and discharge of GR6J for the Jordan River basin at the Sede Nehamia hydrometric station. Analyzes of simulated streamflow were performed both for the 1979–2005 control period and for the 2020–2049 and 2050–2079 future periods (extracted from the continuous 2020–2080 GR6J simulations).

3. Results

3.1. Simulated vs. Observed precipitation for the control period

Table 2 displays the annual precipitation trend for each model vs. the observed slope for the period 1951–2005 using the statistical student's *t*-test It can be seen that the annual precipitation observed trend at Kefar Giladi decreased by -0.14 mm/y for the period 1951–2005. The wide dispersion of the 19 RCMs can be seen in Table 2 and in Fig. 3A-S that displays the observed against the simulated trend for each model. Some of the models show a negative slope (decreasing trend) and other a positive slope, while the range was between -6.56 mm/y (CLMcom_MOHC - MPI-ESM_IMS) to + 4.15 mm/y (CLMcom_MOHC-HadGEM2-ES) and -0.16 mm/y for the ensemble mean. The ensemble mean represents very well the observed precipitation slope with significant P value of 0.01).

Fig. 4 summarizes the precipitation trends and displays the observed precipitation for the period 1951–2005 vs. the ensemble mean for this simulate control period. It shows the larger variability in the observed annual precipitation than in the mean of the ensemble. Fig. 5 displays the monthly precipitation averages of each climate model (A) and the ensemble mean (B) for the period

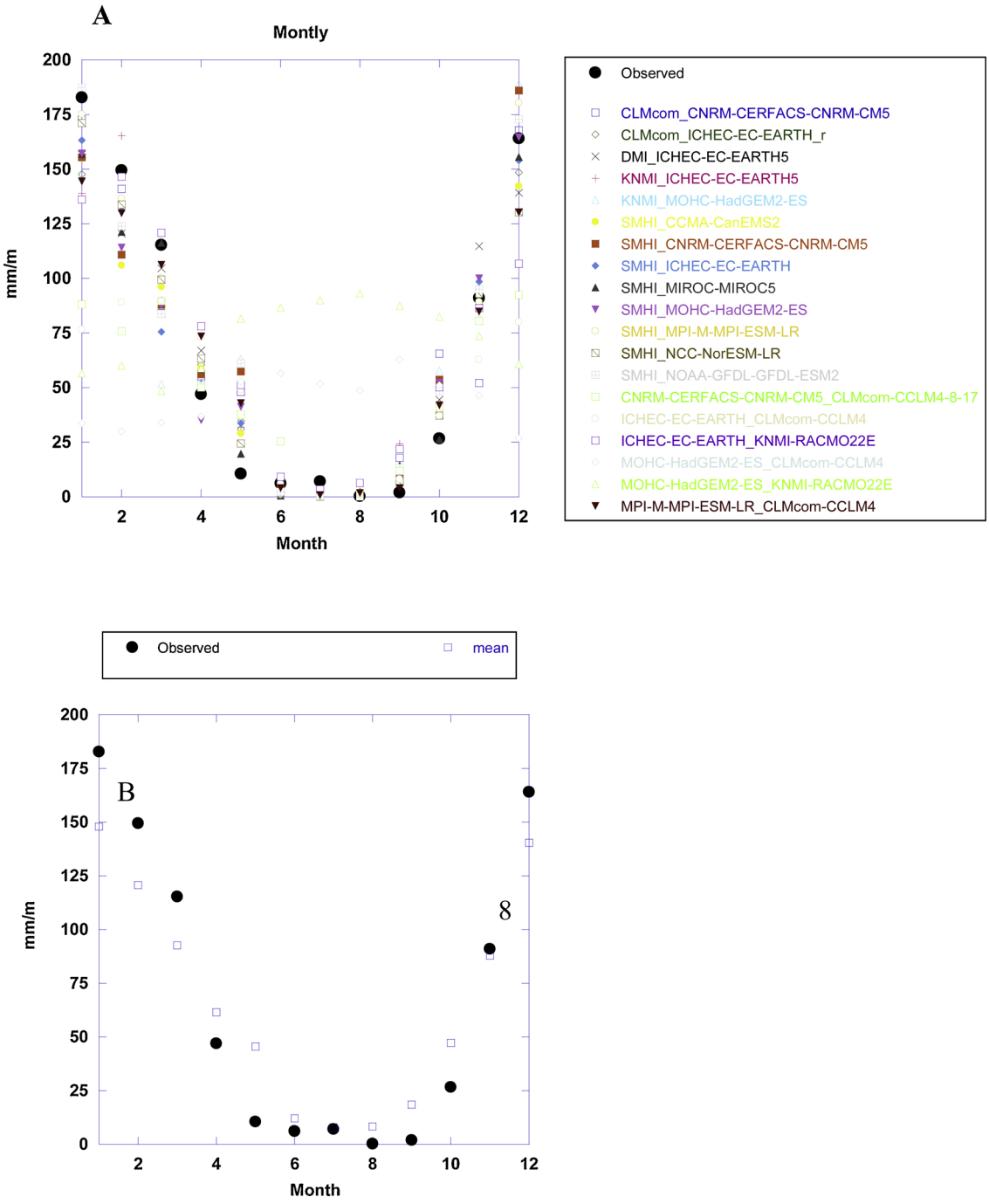

Fig. 5. Simulated monthly precipitation from all models (ensemble mean, in blue) vs. the observed monthly precipitation in Kefar Giladi, Kinnert basin for the control period of 1951–2005.

1951–2005 vs. the observed precipitation values in Kefar Giladi rain gauge. It can be seen that while variability and range differ between the models, the RCM's seasonality fits well to the observed behavior: DJF is the wet season (with precipitation peak in January) and the dry season occurs in JJA (with the lowest amount of precipitation in August).

3.2. Calibration and validation of streamflow volumes at the upper Jordan River using the GR6J hydrological model

Fig. 6 displays observed vs. simulated daily discharge at the upper Jordan River, Sede Nehamia hydrometric station for the calibration period 1981–1987 using the GR6J model (middle and lower panels). The observed precipitation at the Upper Jordan River

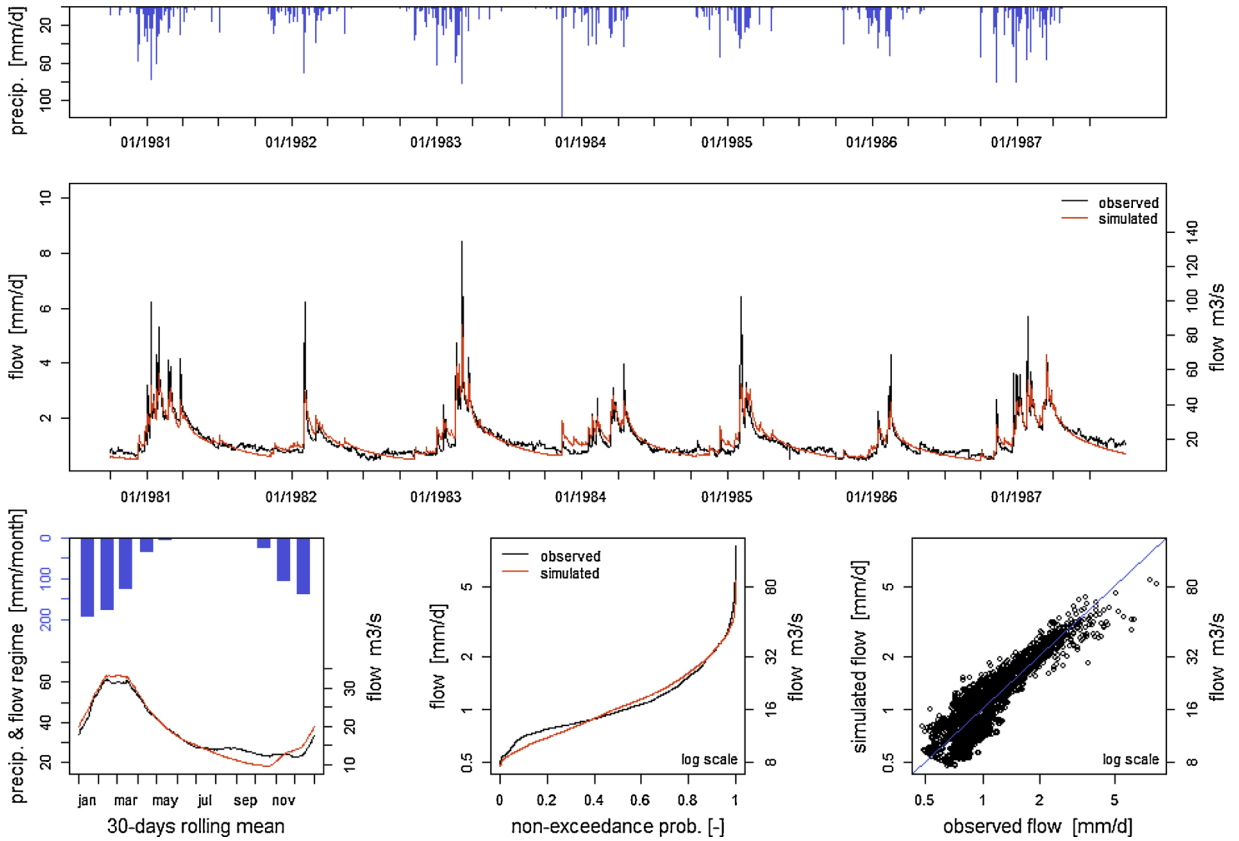

Fig. 6. Observed precipitation at the Upper Jordan River basin (upper panel), observed vs. simulated daily discharge at the Jordan River, Sede Nehemia hydrometric station using the GR6J model (middle and lower panels): results for the calibration period 1981–1987. NSE = 0.82, KGE = 0.91.

basin is shown in the upper panel of the figure. We can observe a slight underestimation of low flows by the model while high flows are generally well reproduced. The results for the calibration period show NSE = 0.82 and KGE = 0.91. Results for the validation period of 1988–2014 (Fig. 7) are lower but still have relatively good agreement with the observed flow: NSE = 0.76 and KGE = 0.84. It can be seen in the model that although there is an overall agreement between the observed and the simulated flows, the model underestimates the high flows in the Jordan River (flood events) and overestimates the low flows at the dry season (June-September) except in a few cases. The inter-annual streamflow regime is globally well reproduced.

These results indicate that GR6J is robust for the Jordan River basin, i.e. that the performance of the model does not drop too much on an independent validation period. As a consequence, the application of GR6J for the present climate change case study can be performed with reasonable confidence about the reliability of the results.

3.3. Future precipitation and potential evapotranspiration trends

Table 3 displays the relative changes in annual precipitation (%) for the near (2020–2049/1979–2005) and far future (2050–2079/1979–2005) periods at the RCP4.5 and RCP8.5 scenarios for each model and for the ensemble mean, compared with the reference period. It can be seen that according to the RCP4.5 ensemble for the near future there is a 3.5% decrease in precipitation and a 11% decrease for the far future, while for the RCP8.5 ensemble the evolution is -10.5% for the near future and -15.5% at the far future. Fig. 8 shows the precipitation trend range at all models for the near future at RCP4.5 and RCP8.5 for the period 1951–2100 and the observed precipitation for the period 1951-2017. Large annual precipitation range can be seen between the various models. We can also observe that the annual mean of the climate projections does not fit well with the observed values, as the annual variability is not well reproduced. This is an expected feature as climate models projections are not intended to represent the chronology of past climate. As a consequence, the average of projections masks the actual projection variability over the years.

Decreasing trends can be seen for both scenarios, with much larger decreasing trends in the RCP8.5 scenario: -1.46 mm/y compared to -0.8 mm/y for RCP4.5.

Fig. 9 (top row) displays the simulated potential evaporation at the upper Jordan River basin for the periods 1951–1978,

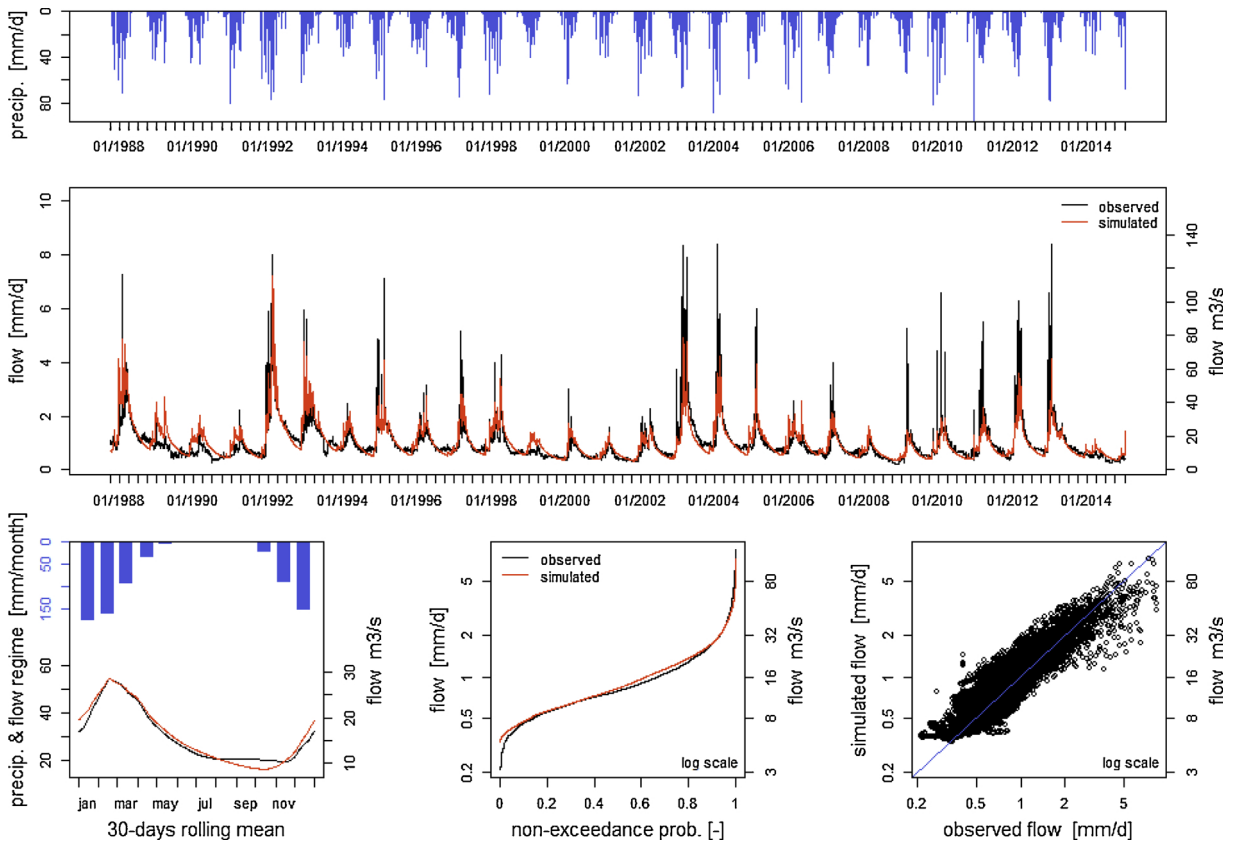

Fig. 7. Same as Fig. 4, but for the GR6J model validation period (1988–2014). NSE = 0.76, KGE = 0.84.

Table 3
Changes in annual precipitation (%) between future and reference periods for all projections.

Model	RCP4.5 2020-2049/ 1979-2005 [%]	RCP8.5 2020-2049/ 1979-2005 [%]	RCP4.5 2050-2079/ 1979-2005 [%]	RCP8.5 2050-2079/ 1979-2005 [%]
Ensemble mean	**−3.4**	**−5.4**	**−9.2**	**−11**
CESM-WRF	−15.6	−17.0	−24.0	−46.8
CLMcom-MPI-ESM	−4.0	−4.0	−11.0	−15.0
CNRM-CNRM-CLMcom-CCLM	+2.0	−7.0	−1.0	−8.0
CLMcom-EC-EARTH	−2.0	+6.0	−3.0	−18.0
KNMI-EC-EARTH	−8.0	–	0.0	–
SMHI_NOAA-GFDL-GFDL-ESM2	−7.4	−7.7	−4.0	−20.3
SMHI_NCC-NorESM-LR	−2.1	−6.6	−11.0	−17.2
SMHI_MPI-M-MPI-ESM-LR	−8.8	+0.4	−17.0	−17.3
CLMcom_CNRM-CERFACS-CNRM-CM5	+0.7	−12.4	−5.0	−21.0
CLMcom_ICHEC-EC-EARTH	−2.6	−3.5	−21.1	−21.8
KNMI_ICHEC-EC-EARTH	+2.3	–	−9.9	–
DMI_ICHEC-EC-EARTH	−10.2	−20.7	−18.4	−25.1
KNMI_MOHC-HadGEM2-ES	−5.8	–	−6.3	–
SMHI_CCMA-CanEMS2	−8.1	−3.6	−9.1	−14.7
SMHI_CNRM-CERFACS-CNRM-CM5	+5.8	−10.3	−0.2	−5.5
SMHI_ICHEC-EC-EARTH	+7.2	+6.0	−1.5	−8.5
SMHI_MIROC-MIROC5	+5.0	+8.7	−8.3	−4.3
SMHI_MOHC-HadGEM2-ES	−10.4	−10.0	−14.6	−17.0

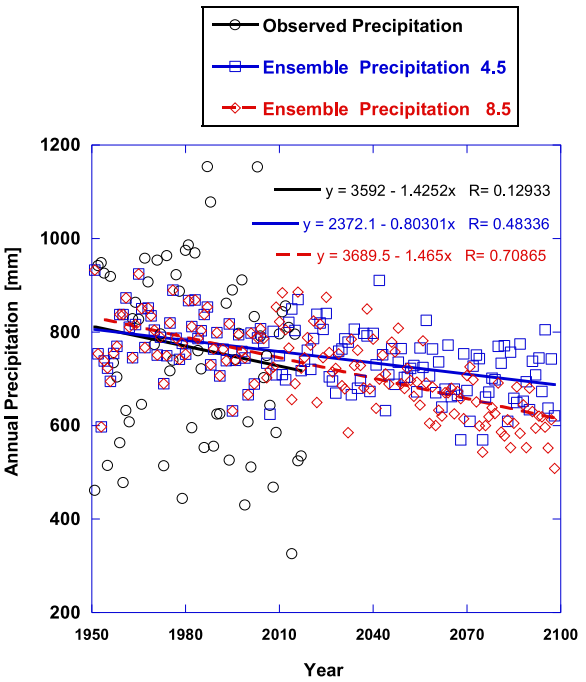

Fig. 8. Simulated annual ensemble precipitation for the period 1951–2100 at the RCP4.5 (blue) and RCP8.5 (red) scenarios. The black line represent the observed precipitation at the Kefar Giladi rain gauge, Kinnert basin.

1979–2010, 2020–2050 and 2071-2098. Increases of 4.6% and 5.4% can be seen in the RCP4.5 scenario for the near and far future respectively (Fig. 9A) and increases of 14.5% and 15.4% can be seen in the RCP8.5 scenario (Fig. 9B). The middle and bottom panels display the same, but for precipitation and stream flow at the Jordan River according to the ensemble mean. Decreases of 2.7% and 7.6% can be seen for precipitation in the RCP4.5 scenario for the near and far future respectively (Fig. 9C) and 5%, 20% respectively (Fig. 9D) can be seen for the RCP8.5 scenario (Fig. 9D). Fig. 9E display the change in stream flow for RCP4.5 scenario (-12.3%, -22% for the near and far future respectively) and 8 F for RCP8.5 (-15.8%, -50% for the near and far future).

Precipitation and evaporation are the major elements in the hydrological cycle and changes in their regimes (decrease in precipitation and increase in evaporation) should have a major effect on the hydrological regime.

3.4. Future streamflow volumes at the Jordan River

Table 4 shows the changes in average annual streamflow (%) for all the models at different periods for the RCP4.5 and RCP8.5 scenarios. It can be seen that according to the ensemble mean the annual streamflow volumes is decreasing by 12% and 22% for the near and far future respectively. For the RCP8.5 scenario, a much more important decrease is expected: 16% and -50% for the near and far future respectively. Again, a wide range of uncertainty can be noted in Table 4 as for the RCP4.5 scenario the annual streamflow ratio with respect to the control period is changing from maximum of +15% to minimum of -28% for the near future and from -3% to -45% for the far future. For the RCP8.5 scenario, the spread of the ratio changes is even larger: from maximum of +9% to minimum of -46% for the near future and from -9% to -51% for the far future. This corroborates the results of Fig. 8 that show how much larger the relative change is for discharge compare to precipitation or actual evapotranspiration in the future.

Fig. 10 illustrates that the decrease of discharge is present for almost all GCMs/RCMs couples and that the decrease is more intense for RCP8.5 than for RCP4.5 and for the far future than for the near future.

Fig. 11shows the annual streamflow at the Jordan River (MCM) for the period 2006–2100 represented by the ensemble mean at RCP4.5 and RCP8.5 scenarios. The strong decreasing trend is striking and it can be observed that RCP8.5 projections indicate lower future discharge. Fig. 12 summarizes the simulation results and displays the change in annual precipitation (%) in respect to the change in annual streamflow (%) for the periods 2020–2049 and 2050–2079 vs. 1979–2005 at the RCP4.5 and RCP8.5 scenarios. It demonstrates very well how streamflow volumes decrease with the decrease in rainfall on a non-linear way, as a decrease of precipitation by 20% can lead to a decrease of stream flow of more than 40% for many projections.

4. Discussion and summary

This study shows new hydroclimate findings for the Upper Jordan River in the northern part of Israel. Israel and the surrounding countries are already experiencing a significant decrease in water availability. The projected trends for precipitation, evapotranspiration and streamflow presented in this study will have major effects for the region, as already indicated by previous studies.

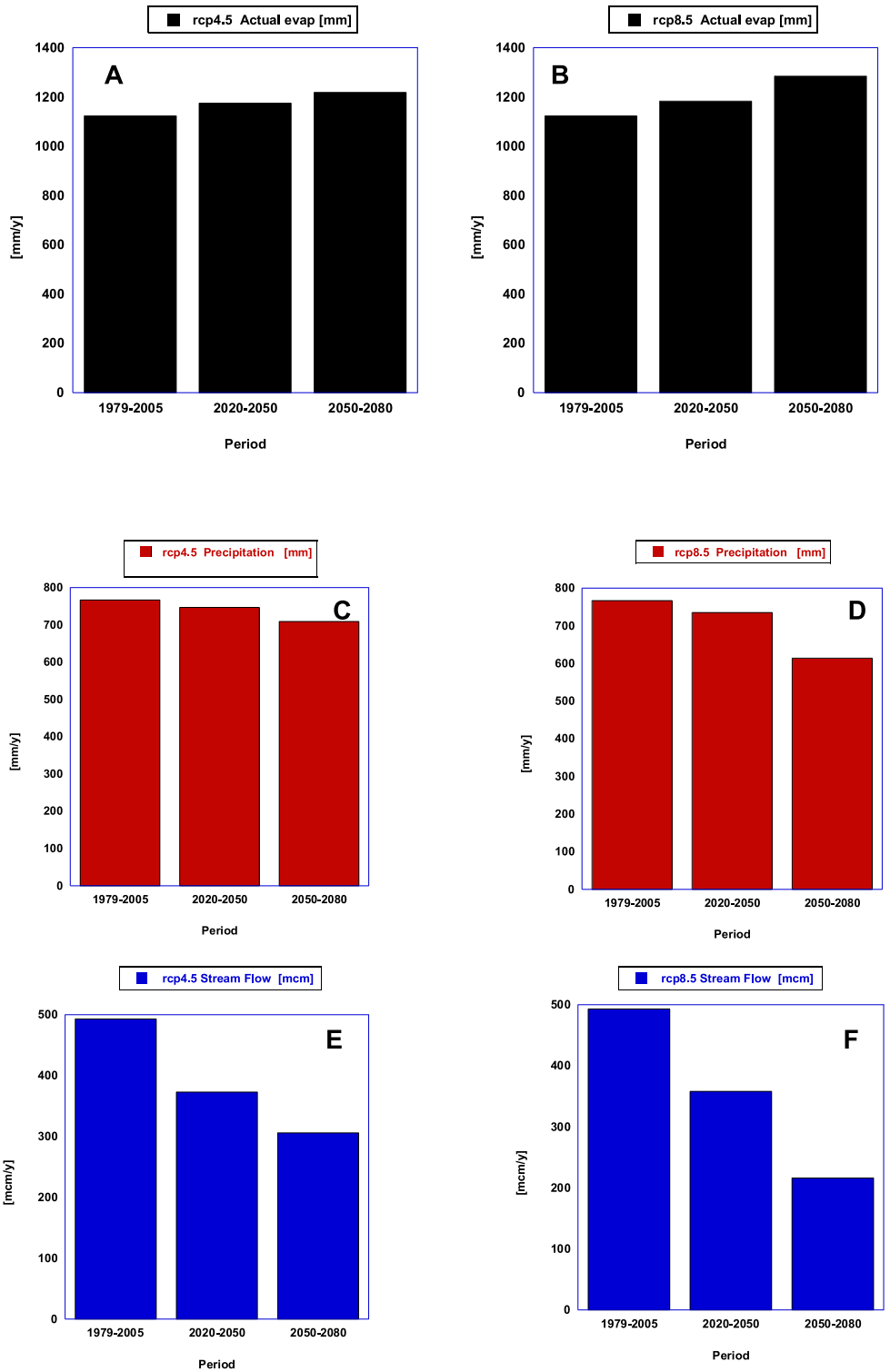

Fig. 9. Annual ensemble mean actual evapotranspiration for the RCP4.5 (blue) and RCP8.5 (red) scenarios (A) and their evolution compared to the control period (B).

In this study, we used for the first time an ensemble of 19 RCMs, some of them having a very high resolution (the Euro Cordex domain). We assessed their trends against observations for a control period of 54 years (1951–2005). Such relatively long time series allow us to robustly quantify each model slope against the observed precipitation slope and to assess our confidence in its results.

Table 4
Changes in annual streamflow (%) between future and reference periods for all projections.

Model	RCP4.5 2020-2049/ 1979-2005 [%]	RCP8.5 2020-2049/ 1979-2005 [%]	RCP4.5 2050-2079/ 1979-2005 [%]	RCP8.5 2050-2079/ 1979-2005 [%]
Ensemble mean	**−10.6**	**−14.5**	**−26.1**	**−35.3**
CESM-WRF	−28.2	−34.3	−39.1	−49.9
CNRM-CNRM-CLMcom-CCLM	+8.0	−6.0	−4.0	−13.0
ICHEC-EC-EARTH-CLMcom-CCLM4	−3.0	+8.0	−4.0	−11.0
MPI-M-MPI-ESM- CLMcom-CCLM	−2.0	−3.0	−3.0	−15.0
SMHI_NOAA-GFDL-GFDL-ESM2	−23.3	−22.0	−29.3	−46.3
SMHI_NCC-NorESM-LR	−14.8	−16.6	−35.8	−35.7
SMHI_MPI-M-MPI-ESM-LR	−25.1	−6.9	−42.4	−43.4
CLMcom_CNRM-CERFACS-CNRM-CM5	−9.1	−31.4	−20.5	−50.1
CLMcom_ICHEC-EC-EARTH	−9.5	−2.4	−45.1	−40.8
KNMI_ICHEC-EC-EARTH	+4.4	–	−19.8	–
DMI_ICHEC-EC-EARTH	−26.2	−46.0	−45.0	−51.2
KNMI_MOHC-HadGEM2-ES	−21.9	–	−33.6	–
SMHI_CCMA-CanEMS2	−24.7	−14.6	−34.7	−43.4
SMHI_CNRM-CERFACS-CNRM-CM5	−0.9	−24.8	−12.5	−26.7
SMHI_ICHEC-EC-EARTH	+9.4	+5.4	−14.1	−27.4
SMHI_MIROC-MIROC5	+15.0	+9.0	−22.5	−25.3
SMHI_MOHC-HadGEM2-ES	−28.2	−31.3	−39.1	−49.7

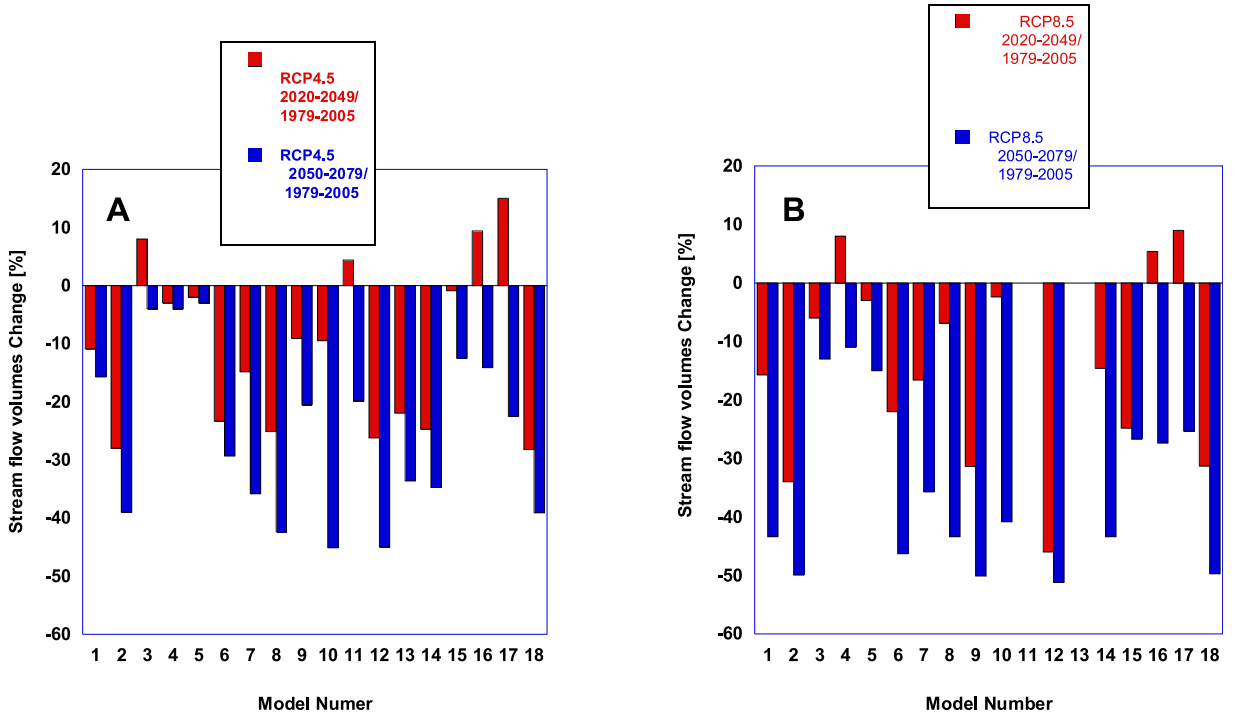

Fig. 10. Future streamflow volume changes at the upper Jordan River at the RCP4.5 (A) and RCP8.5 (B) scenarios for the periods 2020–2049 in respect to 1979–2020 (red) and 2050–2079 in respect to 1979–2005 (blue).

Although there is a large spread between the various models, a decreasing trend in precipitation and increase in evapotranspiration can be seen in the majority of the models, especially for the far future, and for the RCP8.5 scenario. Respectively, the streamflow volumes at the upper Jordan River are decreasing, but in much sharper trend than the precipitation. The results presented in this study show the effects of climate change on water availability by (Table 4) show that a decrease of 4% and 11% in precipitation in the near and far future (RCP4.5) leads to a significant decrease of 11% and 16% in annual stream flow volumes, respectively. For the RCP8.5 scenario a decrease of 5% and 14% in precipitation for the near and far future leads to a decrease of 16%

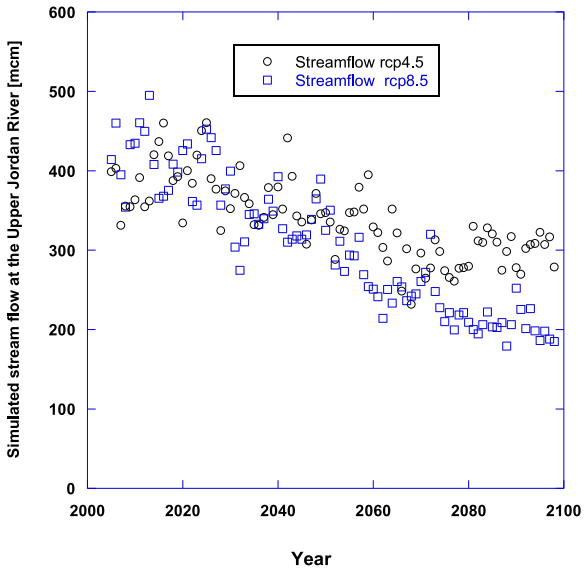

Fig. 11. Ensemble of simulated annual streamflow for the period 2006–2100 at the RCP4.5 (black) and RCP8.5 (blue) scenarios for upper Jordan River, Kinneret basin, using the GR6J model (For interpretation of the references to colour in this figure legend, the reader is referred to the web version of this article).

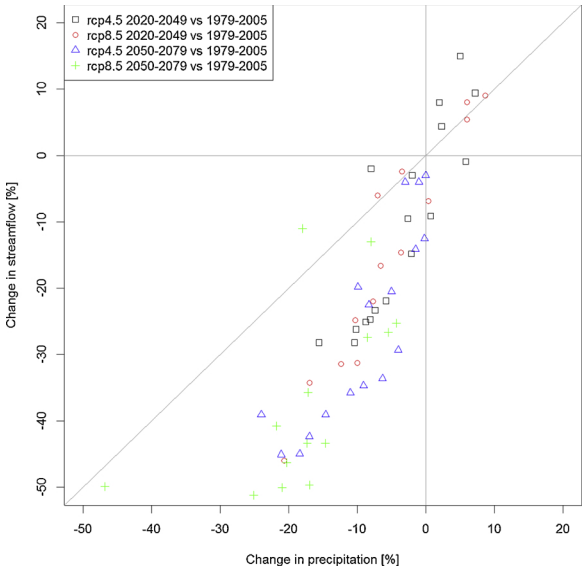

Fig. 12. Change in annual precipitation (%) in respect to the change in annual streamflow (%) for the periods 2020–2049 and 2050–2079 vs. 1979–2005 at the RCP4.5 and RCP8.5 scenarios.

and 44% in the simulated stream flow, respectively. Such trends are dramatic for the region in terms of future water availability and water scarcity. We also suggest that the modification of the rainfall-runoff relationship could lead to enhanced impact of the combined effects of decrease of precipitation and increase of evaporation on the water resources availability.

Using more detailed hydrological models that combine also the effects of changes in land use on the hydrological cycle and water obstructions on downstream flow may sharpen our insight and knowledge of future streamflow. Decision makers will have to decide how to adapt their water sector management based on such climate scenarios and hydrological projections. The results here present the range between the best- and the worst-case scenarios and the ensemble mean. They also provide some clues regarding the quality of each GCM/RCM combination for the control period. Such findings as presented here can help decision makers to better plan the water management with respect to the predicted climate changes.

References

Alpert, P., Price, C., Krichak, S.O., Ziv, B., Saaroni, H., Osetinsky, I., Barkan, J., Kishcha, P., 2005. Tropical tele-connections to the Mediterranean climate and weather. Adv. Geosci. 2, 157–160.

Chenoweth, J., Hadjinicolaou, P., Bruggeman, A., Lelieveld, J., Levin, Z., Lange, M.A., Xoplaki, E., Hadjikakou, M., 2011. Impact of climate change on the water resources of the eastern Mediterranean and Middle East region: modeled 21st century changes and implications. Water Resour. Res. 47https://doi.org/10.1029/2010WR010269. W06506.

Coron, L., Thirel, G., Delaigue, O., Perrin, C., Andréassian, V., 2017a. The suite of lumped GR hydrological models in an r package. Environ. Model. Softw. 94, 166–171. https://doi.org/10.1016/j.envsoft.2017.05.002.

Coron, L., Perrin, C., Delaigue, O., Thirel, G., Michel, C. 2017b. airGR: Suite of GR Hydrological Models for Precipitation-Runoff Modelling. R package version 1.5.0.12. URL: https://webgr.irstea.fr/airGR/.

Evans, J.P., 2009. 21st climate change in the Middle East. Climate Change 92, 417–432.

Fu, C., Wang, S., Xiong, Z., Gutowski, W.J., Lee, D., McGregor, J.L., Sato, Y., Kato, H., Kim, J., Suh, M., 2005. Regional climate model inter comparison project for Asia. Bull. Amer. Meteor. Soc. 86, 257–266.

Givati, A., Rosenfeld, D., 2007. Possible impacts of anthropogenic aerosols on water resources of the Jordan River and the Sea of Galilee. Water Resour. Res. 43https://doi.org/10.1029/2006WR005771. W10419.

Givati, A., Mashor, M., Levi, Y., Paz, D., Carmona, I., Becker, E., 2017. The advantage of using international multi-model ensemble for seasonal precipitation forecast over Israel. Adv. Stat. Climatol. Meteorol. Oceanogr. 2017 Article ID 9204081.

IPCC, 2013. In: Stocker, T.F., Qin, D., Plattner, G.K., Tignor, M., Allen, S.K., Boschung, J., Nauels, A., Xia, Y., Bex, V., Midgley, P.M. (Eds.), Climate Change 2013: The Physical Science Basis. Contribution of Working Group I to the Fifth Assessment Report of the Intergovernmental Panel on Climate Change. Cambridge University Press, Cambridge, United Kingdom and New York, NY, USA. https://doi.org/10.1017/CBO9781107415324. 1535 pp.

Kelley, C.P., Mohtadi, S., Cane, M.A., Seager, R., Kushnir, Y., 2015. Climate change in the Fertile Crescent and implications of the recent Syrian drought. PNAS Early Edition. https://doi.org/10.1073/pnas.1421533112.

Klemeš, V., 1986. Operational testing of hydrological simulation-models. Hydrol. Sci. J. Des Sci. Hydrol. 31 (1), 13–24. https://doi.org/10.1080/02626668609491024.

Kling, H., Fuchs, M., Maria, P., 2012. Runoff conditions in the upper Danube basin under an ensemble of climate change scenarios. Journal of Hydrology 424–425, 264–277.

Kotlarski, S., Keuler, K., Christensen, O.B., Colette, A., Déqué, M., Gobiet, A., Goergen, K., Jacob, D., Lüthi, D., van Meijgaard, E., Nikulin, G., Schär, C., Teichmann, C., Vautard, R., Warrach-Sagi, K., Wulfmeyer, V., 2014. Regional climate modeling on European scales: a joint standard evaluation of the EURO-CORDEX RCM ensemble. Geosci. Model. Dev. Discuss. 7, 1297–1333. https://doi.org/10.5194/gmd-7-1297-2014.

Krichak, S., Alpert, P., Kunin, P., 2010. Numerical simulation of seasonal distribution of precipitation over the eastern Mediterranean with a RCM. Clim. Dyn. 34 (1), 47–59.

Kunstmann, H., Suppan, P., Heckl, A., Rimmer, A., 2007. Regional climate change in the Middle East and impact on hydrology in the Upper Jordan catchment. IAHS Publ. 313, 141–149.

Mearns, L.O., Arritt, R., Biner, S., Bukovsky, M.S., McGinnis, S., Sain, S., Caya, D., Correia, J., Flory, D., Gutowski, W., Takle, E.S., Jones, R., Leung, R., Moufouma-Okia, W., McDaniel, L., Nunes, A.M., Qian, Y., Roads, J., Sloan, L., Snyder, M., 2012. The north american regional climate change assessment program: overview of phase I results. Bull. Amer. Meteor. Soc. 93, 1337–1362. https://doi.org/10.1175/BAMS-D-11-00223.1.

Nash, J.E., Sutcliffe, J.V., 1970. River flow forecasting through conceptual models part I — A discussion of principles. J. Hydrol. (Amst) 10 (3), 282–290. https://doi.org/10.1016/0022-1694(70)90255-6.

Oudin, L., Hervieu, F., Michel, C., Perrin, C., Andréassian, V., Anctil, F., Loumagne, C., 2005. Which potential evapotranspiration input for a rainfall-runoff model? Part 2 – towards a simple and efficient PE model for rainfall-runoff modelling. J. Hydrol. (Amst) 303 (1-4), 290–306. https://doi.org/10.1016/j.jhydrol.2004.08.026.

Peleg, N., Shamir, E., Georgakakos, K.P., Morin, E., 2015. A framework for assessing hydrological regime sensitivity to climate change in a convective rainfall environment: a case study of two medium-sized eastern Mediterranean catchments, Israel. Hydrol. Earth Syst. Sci. Discuss. 19, 567–581. https://doi.org/10.5194/hess-19-567-2015.

Pushpalatha, R., Perrin, C., Le Moine, N., Mathevet, T., Andréassian, V., 2011. A downward structural sensitivity analysis of hydrological models to improve low-flow simulation. J. Hydrol. (Amst) 411 (1-2), 66–76. https://doi.org/10.1016/j.jhydrol.2011.09.034.

Rimmer, A., Givati, A., 2014. In: Zohary, T., Sukenik, A., Berman, T., Nishri, A. (Eds.), “Hydrology”, Chap 7 in “Lake Kinneret – Ecology and Management”. Springer, Heidelberg.

Rimmer, A., Givati, A., Samuels, R., Alpert, P., 2011. Using high resolution climate model to evaluate future water and solutes budgets in the sea of Galilee. J. Hydrol. 410, 248–259.

Saaroni, H., Halfon, N., Ziv, B., Alpert, P., Kutiel, H., 2009. Links between the rainfall regime in Israel and location and intensity of Cyprus lows. Int. J. Climatol DOI: 10.1002/joc.1912.

Samuels, R., Hochman, A., Baharad, A., Givati, A., Levi, Y., Yosef, Y., Saaroni, H., Ziv, B., Harpaza, T., Alpert, P., 2017. Evaluation and projection of extreme precipitation indices in the Eastern Mediterranean based on CMIP5 multi-model ensemble. Int. J. Clim. 1–18. https://doi.org/10.1002/joc.5334.

Shaban, A., 2009. Indicators and aspects of hydrological drought in Lebanon. Water Resour. Manag. 23, 1875–1891.

Smiatek, G., Kunstmann, H., Heckl, A., 2011. High resolution climate change simulations for the Jordan River area. J. Geophys. Res. 116, D16111. https://doi.org/10.1029/2010JD015313.

Solman, S.A., Sanchez, E., Samuelsson, P., 2013. Evaluation of an ensemble of regional climate model simulations over South America driven by the ERA-Interim reanalysis: model performance and uncertainties. Clim. Dyn. 41, 1139. https://doi.org/10.1007/s00382-013-1667-2.

Thirel, G., Andréassian, V., Perrin, C., 2015. On the need to test hydrological models under changing conditions. Hydrol. Sci. J. Des Sci. Hydrol. 60 (7-8), 1165–1173. https://doi.org/10.1080/02626667.2015.1050027.

Eds.). In: Van der Linden, P., Mitchell, J.F.B. (Eds.), ENSEMBLES: Climate Change and Its Impacts: Summary of Research and Results from the ENSEMBLES Project. Met Office Hadley Centre, FitzRoy Road, Exeter EX1 3PB, UK 160pp.

Zittis, G., Hadjinicolaou, P., Lelieveld, J., 2014. Comparison of WRF model physics parameterizations over the MENA-CORDEX domain. Am. J. Clim. Change 3, 490–511.